Influence of large-scale asperities on the stability of concrete dams

Adrian Ulfberg, Jaime Gonzalez-Libreros, Oisik Das, Gabriel Sas, Erik Andersson

Luleå University of Technology, Luleå, Sweden

Dipen Bista[a,b], Bård Arntsen[b], Andreas Seger[b,c]

[a]*Norwegian University of science and technology, Trondheim, Norway*

[b]*SINTEF Narvik, Narvik, Norway*

[c]*The Arctic University of Norway, Tromsø, Norway*

Contact: adrian.ulfberg@ltu.se

Abstract

For concrete dams founded on rock, there are only a few options in the common analysis methods to account for large-scale asperities. However, previous research alludes that they have a significant impact on the behaviour of interfaces under shear. This study investigates the behaviour of concrete dam scale models with varying interface geometries, under a realistic set of eccentric loads. The outcome of the scale model tests shows that not only the capacity of the scale models was significantly impacted by the asperities, but also the type of failure in the scale models.

Keywords: Concrete dams, scale model tests, finite element analysis, digital image correlation

1 Introduction

In accordance with guidelines and standards [1-6], concrete dams are often assessed by analytical methods of calculation. Examples of such methods are the limit equilibrium method or shear friction method for the sliding failure mode, and calculation of the resultant location for the overturning of the dam body. One of the common idealizations these methods require is that considerations regarding displacement are to be neglected [2]. Such an idealization leads to potentially beneficial effects from large-scale asperities, e.g. interlocking between the dam body and foundation to be neglected in the assessment. However, it has been reported that large-scale asperities have a key part in the behaviour of sheared interfaces [7-11]. Also, the location of the large-scale asperity along the interface has a significant influence on the shear capacity of a interface under eccentric loading [12].

When many existing dams were built, the requirements of safety were generally lower [13]. Therefore, the problem that may arise is that the assessment of existing concrete dams may indicate towards insufficient stability. Bearing this in mind, questions regarding the suitability of these analytical methods, for stability assessment arises. These methods may more accurately estimate a concrete dam capacity if, for example, they are further adjusted to account for large variations in the rock-concrete interface. However, before any adjustments are made, a better understanding of these geometrical features of the rock-concrete interface is necessary.

Using experimental testing of four different scale models with varying rock-concrete interface geometries, this study attempted to investigate the effect of large-scale asperities in the rock-concrete interface on the behavior of concrete dams under a realistic set of loads (hydrostatic pressure, ice load, and uplift pressure). The prepared scale models were based on the existing Kalhovd dam, whose recent assessment led to the conclusion that the dam had insufficient stability for the requirement imposed by Norwegian standards [5].

2 Kalhovd dam

Kalhovd dam is a concrete dam and is part of the reservoir Kalhovdfjorden in Norway (Figure 1). It is a 386 m long buttress dam constructed mainly on diorite gneiss type rock and was built between the years 1940-1948 [14]. The centre-to-centre spacing between the individual buttresses is 5 m and the buttress heights vary between 1.5-13.3 m along the dam. The reassessment of the structural safety of the dam, by analytical methods of calculations, concluded that 59 of its buttress sections were unstable in either the overturning failure mode, sliding failure mode, or both. Dam inspections, where the dam geometry was documented using laser scanning technology, were carried out in 2016. The inspection showed that, for most of the buttresses, the rock-concrete interface between the dam and the foundation is uneven. Numerous large asperities in the foundation, in the form of inverted shear keys, were found. The inspection revealed significant differences between the real and assumed dam geometry and foundation topography. Material sampling by core drilling from the dam and foundation was also performed. The material parameter values given from the core samples of the dam are shown in Table 1.

Out of the 59 identified buttress sections with insufficient stability, the buttress section numbered 49 was chosen for the study. It was chosen based on its two, distinguishing, large asperities (2). The cross-sectional image with the various elements of buttress section 49 is shown in Figure 2.

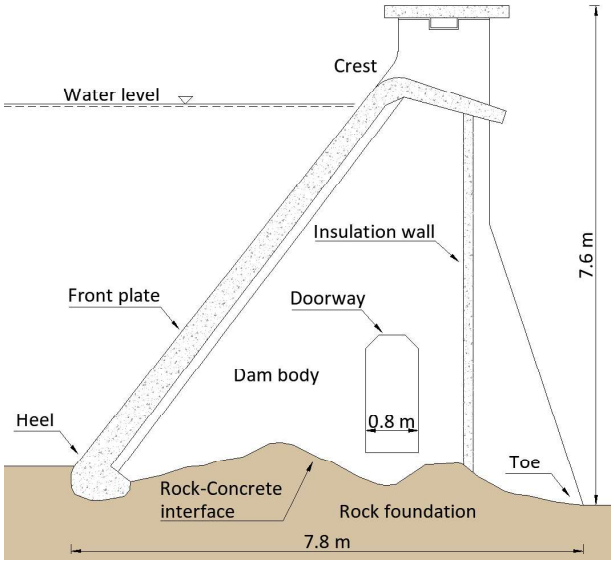

Figure 2. Buttress section 49

3 Method

3.1 Scale model test

Since full-scale testing was unfeasible from an economic standpoint, scale model testing was conducted. Scale model testing is an established analysis method [15], which has been used in testing of various dam structures [16-20]. To investigate the impact of large-scale asperities in the rock-concrete interface on the dam's capacity, four scale models were created. Only the rock-concrete interface geometry differed between the models.

Figure 1. Photograph of dam over Kalhovdfjorden with buttress 49 marked in red

The scale models were named according to whether the geometry included the upstream (UA) or downstream asperity (DA), and the model which included the large-scale upstream and downstream asperity was named UDA (Upstream Downstream Asperity). One model without any large-scale asperity was cast and was named R (reference) model. This R model has a geometry equivalent to the assumed geometry in the stability assessment by the analytical models. The models with their respective rock-concrete interfaces are shown in Figure 1.

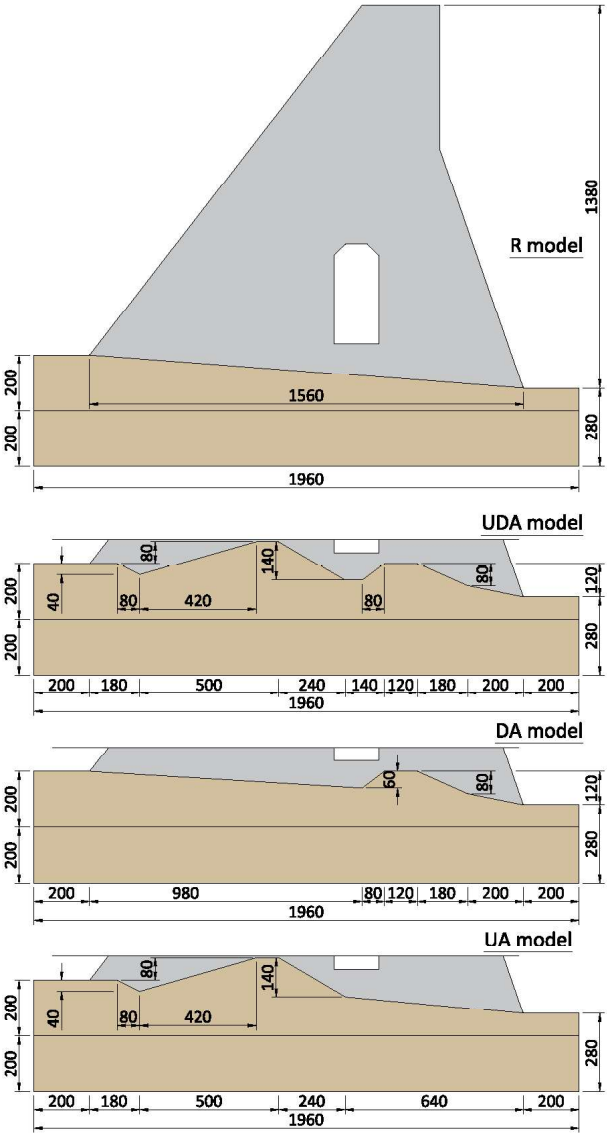

Figure 1. Geometries of scale models

The front plate and the insulation wall were not included in the scale models as the only geometrical differences between the scale models are in the rock-concrete interfaces. The foundations were casted from equivalent C30/37 type concrete and the buttress scale models were match casted against the foundation. The bond between the buttress scale model and foundation was broken by application of rubber paint, which was scraped off before testing. The models were scaled down 1:5 from the prototype (i.e. real structure) using similitude theory [21].

3.1.1 Scaling of the models

Conforming to the similitude theory, material parameters were scaled down. The material properties of the scaled down models are related by equations (1), (2), and (3):

$$\frac{S_\sigma}{S_\rho S_L} = 1 \tag{1}$$

$$S_\varepsilon = S_\rho = S_\nu = 1 \tag{2}$$

$$\frac{S_\sigma}{S_E} = \frac{S_s}{S_L} = \frac{S_\sigma}{S_f} = 1 \tag{3}$$

The symbol *S* is the scaling factor and the subscript letters σ, *L*, ρ, ε, ν, *E*, *s*, and *f* denote the stress, geometry, density, strain, Poisson's ratio, modulus of elasticity, displacement, and strength parameters, respectively. Based on these scaling laws, the ideal scale without any distortions would have material parameters corresponding to Table 1.

Table 1. Material properties of buttress prototype and ideal scale model

Material parameter	Prototype	Ideal scale model
Cylinder compressive strength, f_c [MPa]	33.0	6.6
Tensile strength, f_t [MPa]	4.0	0.8
Initial modulus of elasticity, E_0 [GPa]	26.3	5.2
Secant modulus of elasticity, E_C [GPa]	25.2	5.0
Strain at crushing, ε_{fc} [‰]	2.01	2.01
Friction angle, φ [°]	36.2	36.2
Density, ρ [kg/m^3]	2354	2354

The mortar mix that was chosen for the scale models of the buttress used a mix 1:0.6:3 of cement, water, and sand (0-4 mm). Ten cylinders were cast from each scale model mortar mix and the average values from the material parameter tests are shown in Table 2. Values in parentheses in Table 2 are the coefficients of variation.

Table 2. Average material properties for scale models

	Scale model			
Material parameter	**R**	**UDA**	**DA**	**UA**
Cylinder compressive strength, f_c [MPa]	12.1 (2%)	10.0 (0.5%)	7.9 (2%)	9.4 (0.5%)
Tensile strength, f_t [MPa]	1.2 (3%)	0.8 (3%)	0.8 (8%)	0.8 (4%)
Initial modulus of elasticity, E_0 [GPa]	11.3 (6%)	10.7 (3%)	10.2 (8%)	10.3 (1%)
Secant modulus of elasticity, E_C [GPa]	10.9 (9%)	10.1 (5%)	8.3 (2%)	9.6 (1%)
Strain at crushing, ε_{fc} [-]	3.06 (6%)	2.46 (13%)	1.95 (5%)	2.33 (1%)
Friction angle, φ [°]	37.9 (3%)	35.6 (4%)	35.6 (4%)	36.1 (2%)

Deviations between the ideal scale models material parameters can be seen. However, this was considered to only affect the results slightly as failure in the buttress scale model material was considered unlikely for the intended loading scheme (section 3.1.3). Instead, the friction angle, which only saw small deviations, was assumed to be the most impactful material property for the tests. Along with the material parameters, the loads for the prototype had to be scaled down, as well. These design loads for the prototype are given in Table 3 with the equivalent scaled loads. The ideal scale model pressures converted to loads are shown in parentheses in Table 3.

Table 3. Design loads acting on buttress prototype and ideal scale model

Load type	**Prototype**	**Ideal scale model**
Hydrostatic pressure [kPa]	61.1	12.2 (9.3 kN)
Uplift pressure [kPa]	61.1	12.2 (0.76 kN)
Ice pressure [kPa]	500	40 (4 kN)

3.1.2 Test setup

The test setup consisted of a loading system and a guiding and restraining system. Figure 2, displays the test setup with the UDA model and its foundation. The foundations of the scale models were anchored to a strong floor to prevent them from sliding. Restraints were used to keep the scale models in-plane during testing. Linear variable differential transformers (LVDTs) were among the measuring tools (described further in section 3.1.4) used and the LVDT measuring the horizontal crest displacement is shown in Figure 2.

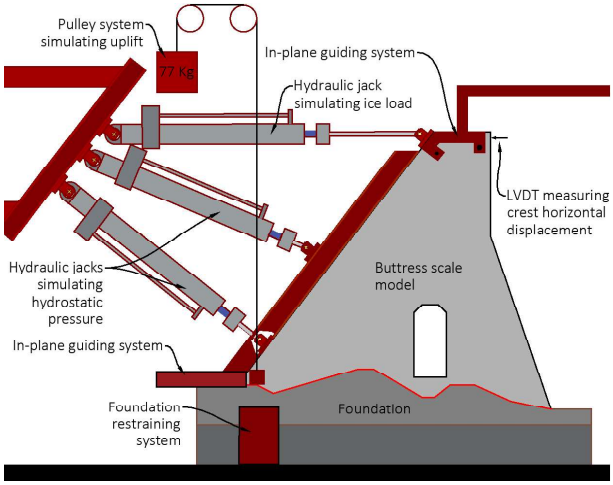

Figure 2. Schematic diagram of the test setup

The loading system consisted of two hydraulic jacks intended to simulate the hydrostatic pressure acting on the prototype. The load ratio between the two jacks was constantly kept at 0.45:0.55, where the hydraulic jack located furthest down applied the highest load. These two jacks were attached to a HEA 100 loading beam to distribute the two point-loads from the jacks into a triangular pressure, equivalent to that of hydrostatic pressure acting on the prototype. A rubber mat was placed in between the loading beam and the buttress scale models to better transfer the pressure.

A third hydraulic jack was used to simulate the ice load at the crest of the dam. To simulate the uplift pressure, assuming to act only at the front plate as described by [5], a weight of 77 kg was hung with a pulley system attached to the heel of the scale model. Extra weight was added to the scale model to account for the differences in densities between the ideal scale model and the casted scale models.

3.1.3 Loading sequence

The loading scheme for the tests were as follows: First, the hydrostatic pressure was applied followed by the uplift, and finally, the ice load was applied.

3.1.4 Instrumentation and monitoring

The buttress' displacements was monitored by using LVDTs in areas of interest (e.g. along the interface to measure the tangential and perpendicular displacements). Most importantly, for this study, is the LVDT measuring the horizontal displacement at the crest (seen in Figure 2) of the buttress scale models. The measurement from the LVDT at the crest is used to plot the load-displacement diagram shown in section 4. Digital image correlation (DIC) was also used to measure the displacement and strains in the scale models.

4 Results

The load-displacement diagrams from the experimental tests of the buttress scale models are shown in Figure 3.

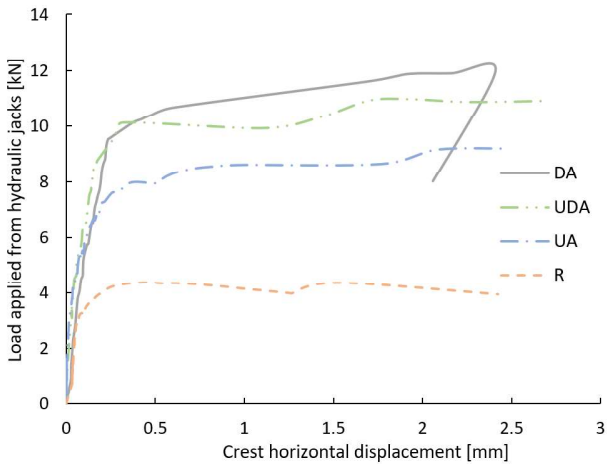

Figure 3. Load-displacement diagram for buttress scale models

The scale models with the highest capacity are in order of DA, UDA, UA, and R. The DA model had a capacity of 12 kN of total applied load whereas the worst performing model, R, which included no asperities, withstood only 4 kN. Models UA and R failed during the application of the equivalent hydrostatic force and no uplift or ice load could be applied. The loads applied during testing of the individual buttress scale models is shown in Figure 4.

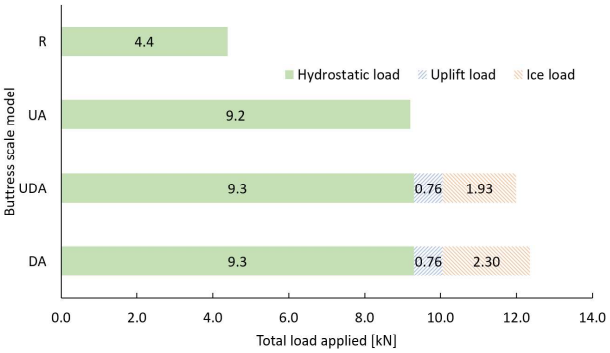

Figure 4. Type and magnitude of applied loads before failure of scale models

The behaviour of the scale models during loading depended on the back asperity. For the buttress scale models which did not include the back asperity, UA and R, the scale model progressively displaced parallel to the interface. The ratio of displacement and applied load progressively increased near failure. The UA model's global displacement was tangential to the upstream asperity's face closest to the applied load. The R buttress scale model's global displacement tangent its straight interface.

The global displacement from the DIC measurements of the UA model at failure is shown in Figure 5. Note that the image of the buttress scale model is mirrored, and the hydraulic jacks is to the right in the figure (previously depicted on the left side of the scale model).

The models UDA and DA, which included the back asperity, only saw slight displacement along the interface for the equivalent hydrostatic load. As the ice load was applied, rotation of the scale models could be seen with the pivot at the beginning of the back asperity. Nearing the failure load, increased sliding could be seen tangential to the back asperities face on the loaded side. The behaviour of the UDA and DA model during the loading suggest that the buttress scale models interlock with the foundation when the downstream asperity is included. The global displacement from the DIC measurements of the DA model at failure is shown in Figure 6.

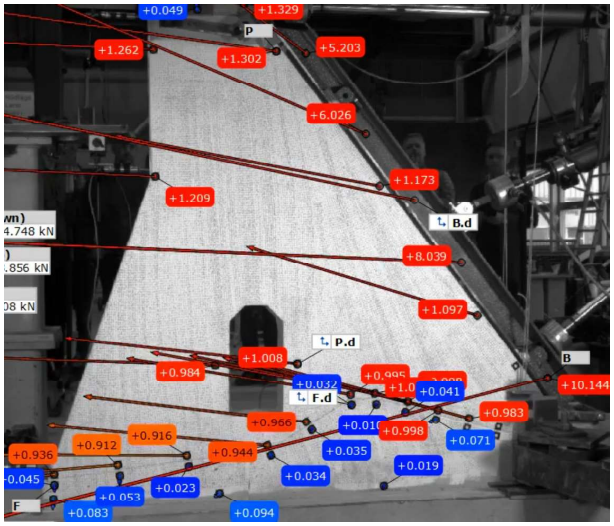

Figure 5. Global displacement [mm] from DIC at failure of buttress scale model UA

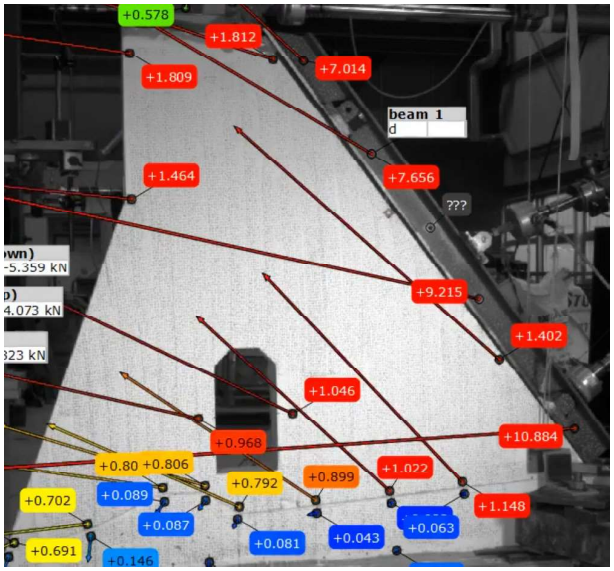

Figure 6. Global displacement [mm] from DIC after failure of buttress scale model DA

5 Analysis and discussion

The results from the scale model tests show that the asperities in the rock-concrete interface had a significant impact on the capacity of each buttress scale model. In relation to the buttress scale model R, which has a geometry equivalent to that of the commonly assumed geometry in analytical assessment, a factor of two was gained in capacity when including the upstream asperity. When including the downstream asperity, the increase in capacity was almost thrice that of the buttress scale model R (if no distinction between the loads is made).

The effect of including both the upstream and downstream asperity is, however, not cumulative on the capacity since the UDA model had a lower capacity than the DA model. This is caused by the decrease in the volume of the buttress, resulting in less stabilizing moment to counteract the rotation of the buttress scale models close to failure. This rotation that can be seen in the models UDA and DA (that include the downstream asperity) is linked to the interlocking that could be seen between the buttress scale models and the downstream asperity. With the size difference between the downstream and upstream asperity, interlocking is most likely not caused by the size of the asperity, but rather the inclination. This inclination results in greater load transfer through normal forces in the rock-concrete interface at the downstream asperity instead of shear. Further, due to interlocking, no conclusions can be drawn regarding the effect of asperity location along the interface.

Even without the effect of interlocking, the buttress scale model UA, containing the large upstream asperity, significantly increased the capacity. This is also likely due to more normal stresses in the interface due to the inclination of the asperity, resulting in development of higher shear resistance in the rock-concrete interface.

The buttress scale models did not include the front plate nor any reinforcement or rock bolts that are present in the prototype (i.e. real structure). Inclusion of these in the buttress scale models would likely increase the capacity further for all the tested models and would be an interesting potential future study. The increase in capacity from these features, on each scale model presented in this paper, may not be a constant value since the failure mechanisms varied depending on the geometry of the rock-concrete interface.

6 Conclusions

Using scale model testing, the aim of the study was to investigate the impact of large-scale asperities in the rock-concrete interface on the capacity of concrete dams under a realistic load setting.

The results from the scale model tests show that the capacity greatly increases by inclusion of large-

scale asperities in the rock-concrete interface. Not only was the capacity governed by the large-scale asperities but also the overall behaviour of the buttress scale models.

Models including the smaller downstream asperity, with higher inclination, interlocked with the foundation and eventually failed as rotations increased. The model that included the larger upstream asperity with less inclination failed comparable to that of the model which did not include any asperities, but, at a substantially higher load.

The results imply that there may be an extra capacity in concrete dams with uneven rock-concrete interface. This capacity may be hidden from the analytical assessment methods, that are commonly used today, without modifications to directly account for large-scale asperities.

7 Acknowledgements

The authors are grateful for the funding from the "The Stable Dams" project with the grant number 244029 and FORMAS with grant number 2019-01236. The authors also express their gratitude to the research program council of Norway, ENERGIX.

8 References

[1] ANCOLD. Guidelines on design criteria for concrete gravity dams. Australian National Committee on Large Dams; 1991.

[2] USACE. Gravity dam design. US Army Corps of Engineers; 1995.

[3] CFGB. Small dams - Guidelines for Design, Construction and Monitoring. French Committee on Large Dams; 2002.

[4] IS. Criteria for design of solid gravity dams. IS: 6512-2003. 2003. Report No.: IS 6512.

[5] NVE. Retningslinjer for betongdammer til § 4.8 i forskrift om sikkerhet og tilsyn med vassdragsanlegg. Norges vassdrags og-energidirektorat, Directorate NWRaE; 2005.

[6] FERC. Engineering Guidelines for the Evaluation of Hydropower Projects: 3 Federal Energy Regulatory Commission; 2016.

[7] D. PF. Multiple modes of shear failure in rock. Proceedings of the 1st international congress of rock mechanics: International Society for Rock Mechanics; 1966.

[8] Grasselli G. Shear strength of rock joints based on quantified surface description [PhD thesis]: École polytechnique fédérale de Lausanne; 2001.

[9] Asadi MS, Rasouli V, Barla G. A Laboratory Shear Cell Used for Simulation of Shear Strength and Asperity Degradation of Rough Rock Fractures. Rock Mechanics and Rock Engineering. 2013;46(4):683-99.

[10] Gravel C, Moradian OZ, Fathi A, Ballivy G, Quirion M. In Situ Shear Testing of Simulated Dam Concrete-Rock Interfaces. 2015.

[11] Zhang X, Jiang Q, Chen N, Wei W, Feng X. Laboratory Investigation on Shear Behavior of Rock Joints and a New Peak Shear Strength Criterion. Rock Mechanics and Rock Engineering. 2016;49(9):3495-512.

[12] Dipen B, Gabriel S, Fredrik J, Leif L. Influence of location of large-scale asperity on shear strength of concrete-rock interface under eccentric load. Journal of Rock Mechanics and Geotechnical Engineering. 2020;12(3):449-60.

[13] Westberg Wilde MJ, F, editor Probabilistic model code för betongdammar. SwedCOLD; 2017.

[14] Gabriel S, Cosmin P, Dipen B, Andreas S, Bård A, Fredrik J, et al. Influence of large-scale asperities on the shear strength of concrete-rock interface of small buttress dams. Engineering Structures. 2021;245:112952.

[15] Harris HGS, G M. Structural Modelling and Experimental Techniques. 2 ed. Boca Raton, Florida: CRC Press; 1999.

[16] Barpi FV, S. Numerical Simulation of Prenotched Gravity Dam Models. Journal of Engineering Mechanics. 2000;126(6):611-9.

[17] Liu J, Feng X-T, Ding X-L, Zhang J, Yue D-M. Stability assessment of the Three-Gorges Dam foundation, China, using physical and numerical modeling—Part I: physical model tests. International Journal of Rock Mechanics and Mining Sciences. 2003;40(5):609-31.

[18] Harris DTF. Investigation of the Failure Modes of Concrete Dams - Physical Model Tests. U.S. Department of the Interior Bureau of Reclamation; 2006. Contract No.: DSO-06-03.

[19] Zhu HHYJ-HD, J-H; Zhang, L Physical Modelling of Sliding Failure of Concrete Gravity Dam under Overloading Condition. Geomechanics and Engineering. 2010;2:89–106.

[20] Chen YZ, L; Yang, B; Dong, J; Chen, J. Geomechanical model test on dam stability and application to Jinping High arch dam. International Journal of Rock Mechanics and Mining Sciences. 2015;76:1-9.

[21] Buckingham E. On Physically Similar Systems; Illustrations of the Use of Dimensional Equations. Physical Review. 1914;4(4):345-76.